

Accumulation of ambient phosphate into the periplasm of marine bacteria is proton motive force dependent

Nina A. Kamennaya^{1,2,5}, Kalotina Geraki³, David J. Scanlan² & Mikhail V. Zubkov^{1,4}✉

Bacteria acquire phosphate (P_i) by maintaining a periplasmic concentration below environmental levels. We recently described an extracellular P_i buffer which appears to counteract the gradient required for P_i diffusion. Here, we demonstrate that various treatments to outer membrane (OM) constituents do not affect the buffered P_i because bacteria accumulate P_i in the periplasm, from which it can be removed hypo-osmotically. The periplasmic P_i can be gradually imported into the cytoplasm by ATP-powered transport, however, the proton motive force (PMF) is not required to keep P_i in the periplasm. In contrast, the accumulation of P_i into the periplasm across the OM is PMF-dependent and can be enhanced by light energy. Because the conventional mechanism of P_i -specific transport cannot explain P_i accumulation in the periplasm we propose that periplasmic P_i anions pair with chemiosmotic cations of the PMF and millions of accumulated P_i pairs could influence the periplasmic osmolarity of marine bacteria.

¹National Oceanography Centre, Southampton SO14 3ZH, UK. ²School of Life Sciences, University of Warwick, Gibbet Hill, Coventry CV4 7AL, UK.

³Diamond Light Source Ltd, Harwell Science and Innovation Campus, Chilton, Didcot OX11 0DE, UK. ⁴Scottish Association for Marine Science, Scottish Marine Institute, Oban, Argyll PA37 1QA, UK. ⁵Present address: School of Plant Sciences and Food Security, The George S. Wise Faculty of Life Sciences, Tel Aviv University, Tel Aviv 6997801, Israel. ✉email: Mikhail.Zubkov@sams.ac.uk

Phosphorus (P) is a macronutrient universally required by all organisms including bacteria. Bacteria have a number of ways to acquire P. Scavenging P from organic molecules and reducing growth dependence on P by substituting P with sulfur in their membranes^{1–6} are both beneficial for bacteria living in phosphate (P_i)-depleted marine environments. However, there is compelling evidence that bacteria prefer P_i to organic P molecules^{7–9}. Marine bacteria, which typically have two membranes (and therefore stain Gram negative), acquire P_i using a diffusion gradient between the environment and the periplasm^{10,11}. In their cells, the periplasm is separated from the environment by the outer membrane (OM), whose permeability to small, hydrophilic solutes is controlled mainly by hydrated channels—porins (Fig. 1a†). Porins select solutes on the basis of their size, shape and charge^{12,13}. When nutrients such as P_i

become depleted, cells increase the number of porins to facilitate nutrient diffusion¹⁴.

There are the three known bacterial transport systems to import P_i from the periplasm into the cytoplasm: a low affinity-high velocity phosphate inorganic transport (Pit) system, a low affinity-high velocity Na-dependent phosphate transport (Npt) system and a high affinity-low velocity phosphate-specific transport (Pst) system^{15–17}. Bacteria living in P_i -depleted waters use only the Pst system^{18,19}. The PstCAB transporter is ATP-powered and receives P_i from a carrier protein, a PstS subunit, when the latter docks at its periplasmic side (Fig. 1a†). Although the P_i concentration of $\sim 10^{-7} \text{ mol l}^{-1}$ required for efficient import of P_i by PstSCAB²⁰ is relatively high, it should not restrict P_i diffusion into the periplasm, because the periplasmic volume of even a relatively large bacterial cell, e.g., *Synechococcus*

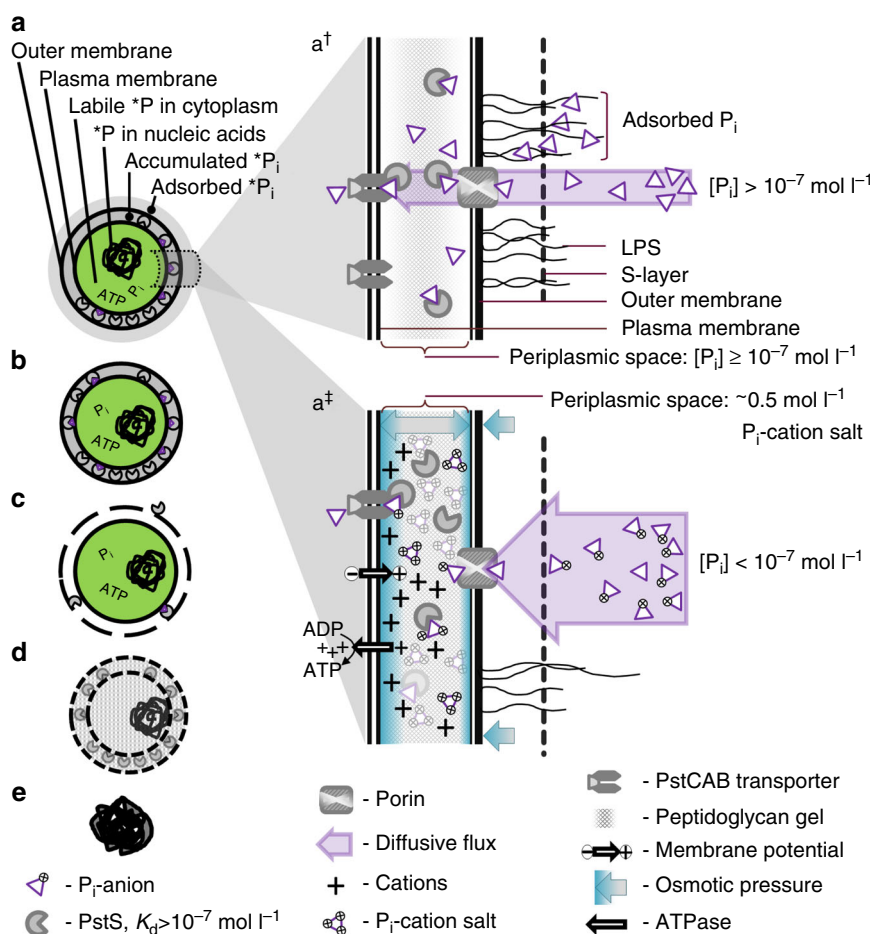


Fig. 1 Phosphate (P_i) acquisition by marine bacteria. **a** In a model cell labelled with *P_i the *P_i -tracer can be (i) extracellular, i.e., adsorbed onto the cell surface; (ii) accumulated in the periplasm; (iii) bound to the PstS subunit in the periplasm; (iv) in a labile form in the cytoplasm, e.g., soluble P_i , nucleotides, sugar phosphates, small molecules of RNA; and (v) in a non-labile form of assimilated P, e.g., DNA, ribosomal RNA, polyphosphates, phospholipids. **a†** Current understanding—parallel processes of passive adsorption of P_i to the bacterial cell surface composed of polymers of the outer membrane lipopolysaccharide (LPS) and overlaid (in some bacteria) by the proteinaceous surface layer (S-layer) and P_i diffusion across the outer membrane through porins into the periplasm. Diffusion is coupled directly to P_i transport across the cytoplasmic membrane by ABC-type transporters (PstCAB) using the periplasmic P_i -binding protein (PstS). **a‡** The proposed model—mass transfer of P_i anions across the outer membrane through porins, their buffering by cations of the membrane potential in the periplasm and import of P_i from the buffered stock through the cytoplasmic membrane by PstCAB using P_i -PstS. Isotonic or slightly hypertonic osmotic pressure is maintained in the periplasm by the buffered P_i salt. **b–e** Removal of different phosphorus pools by washing or fixation of a model *P_i -labelled *Synechococcus* cell. **b** Treatment with surfactants, hydrolytic enzymes and amended ASW removes the extracellular P_i adsorbed to cell surface constituents. **c** A short wash with hypotonic solution, e.g., deionized water (DW), dissolves the extracellularly adsorbed P_i and, by causing osmotic shock, releases the periplasmic contents of a cell, i.e., the accumulated and PstS-bound P_i . **d** Fixation of cells with paraformaldehyde (PFA) compromises the outer and inner membranes, releasing labile periplasmic and intracellular P_i , but crosslinks cellular proteins, immobilizing the primary phosphorus-containing macromolecules including DNA, rRNA and P_i -carrying PstS subunits. **e** Fixation of cells with trichloroacetic acid (TCA) disrupts membranes and precipitates cellular macromolecules (proteins, nucleic acids, polyphosphates and polysaccharides), thereby releasing labile P_i but immobilizing most of the assimilated P_i .

cyanobacteria (Supplementary Table 1) with an estimated periplasmic depth²¹ of 10^{-8} m, is only about 2×10^{-17} l. In such a tiny volume, the presence of only a few free P_i molecules would exceed the threshold 10^{-7} mol l⁻¹ P_i concentration (Fig. 1a†).

Bacteria maximize the diffusive flux of nutrients through the OM by maintaining a steep nutrient concentration gradient between the environment and periplasm^{10,11}. Consequently, to allow efficient diffusion of P_i into the periplasm in P_i -depleted (10^{-9} – 10^{-8} mol l⁻¹) oceanic surface waters^{7,22}, the periplasmic P_i concentration should hypothetically be $<10^{-9}$ mol l⁻¹. This means that there should be no free P_i molecules in the periplasm, i.e., every P_i molecule entering the periplasm should be instantly bound by a PstS subunit requiring an affinity >100 times above the known PstS affinity limit. However, the PstS affinity requirement does not seem to limit the growth of ubiquitous SAR11 alphaproteobacteria and *Prochlorococcus* cyanobacteria—the two bacterial populations comprising $\leq 3/4$ of oceanic surface bacterioplankton in the P_i -depleted North Atlantic subtropical gyre⁷. Furthermore, the ecological success of these bacteria is probably related to the high rates of P_i uptake measured in the gyre^{7,22}. Surprisingly, measured rates of P_i acquisition by *Prochlorococcus* and SAR11 are lower in tropical surface waters where bacterial growth and P_i concentrations are higher²². The counter-intuitive reduction in the P_i acquisition rate by faster growing bacteria was attributed to the presence of an intermediate buffer, in which both SAR11 and *Prochlorococcus* cells store P_i : the fuller the P_i buffer is, e.g., in P_i -replete tropical surface waters, the fewer P_i molecules a cell acquires slower from seawater to top the buffer up²². As every P_i molecule acquired, or more precisely accumulated, by a cell first enters the buffer before being imported for assimilation, bacterial P_i uptake into the buffer and P_i import from the buffer can be decoupled. Although *Prochlorococcus* and SAR11 bacteria possess genes related to synthesis of polyphosphates²³, their cells are perhaps too small to store P_i as polyphosphates intracellularly and they somehow accumulate P_i extracellularly.

Our aim here is to explain how marine bacteria accumulate P_i extracellularly. We demonstrate that P_i accumulation rates by oceanic SAR11, *Prochlorococcus* and *Synechococcus* cells are extremely variable in the P_i -depleted North Atlantic. Lower rates can be stimulated by light energy but their maximal rates are insensitive to light and approach the theoretical upper limit of diffusion. To relate the accumulated P_i with cellular P_i requirements, the P contents of flow-sorted cells of oceanic *Prochlorococcus* and SAR11 were determined by microbeam synchrotron X-ray fluorescence (μ -SXRF) using flow-sorted cultured *Synechococcus* cells for calibration. Using pulse-chase experiments with ³³P_i and ³²P_i (*P_i) radiotracers, we showed that cultured *Synechococcus* cells accumulate P_i in a similar way to SAR11 and *Prochlorococcus* cells²². This justified the use of *Synechococcus* isolates for more intrusive tests (e.g., of retention of accumulated P_i), to curtail artefacts resulting from the low tolerance of oceanic SAR11 and *Prochlorococcus* bacteria to harsh experimental manipulations. Moreover, by working with artificial seawater (ASW), we expanded the experimental range of P_i concentrations below those encountered in natural P_i -depleted seawater. To examine how the extracellular P_i is retained, we developed a living cellular model system with the extracellular *P_i-labelled buffer (Fig. 1a) and treated them with hydrolytic enzymes, surfactants, inhibitors, amended ASW and hypotonic solutions to locate whether the P_i buffer is on the cell surface (Fig. 1b), e.g., retained by a charged S-layer, as was recently proposed for archaea²⁴, or in the periplasm (Fig. 1c). We used specific metabolic inhibitors^{25–28} to determine whether the proton motive force (PMF) is driving extracellular P_i accumulation and retention.

Based on our field and laboratory experiments, we conclude that the PMF is essential for P_i accumulation (but not retention) in the periplasm of marine bacteria. As the PstS-driven import cannot explain P_i accumulation in the periplasm, we propose a mechanism of periplasmic ionic pairing of inwardly diffusing P_i anions with chemiosmotic cations of the membrane potential (Fig. 1a†), which could conserve cellular energy and control periplasmic turgor.

Results

Bacterial clearance rates of P_i . P_i clearance rates (the volume of water cleared of P_i by a cell per unit of time, while the cell accumulates the cleared P_i) of oceanic SAR11, *Prochlorococcus* and *Synechococcus* cells vary by orders of magnitude in the patchily P_i -depleted North Atlantic (Supplementary Figs. 1 and 2a, and Supplementary Table 2). Living in such a patchy environment warrants the use of an extracellular buffer, where P_i is temporarily stored²². Mostly the measured rates are lower in waters adjacent to the subtropical gyre with higher in situ P_i concentrations, whereas the rates are higher in the central gyre waters with lower P_i concentrations (18–28°N, Supplementary Fig. 2a and Supplementary Table 2). In the central gyre waters, maximal P_i clearance rates of SAR11, *Prochlorococcus* and *Synechococcus* cells (Fig. 2a) are only 30×, 40× and 25×, respectively, below the theoretical maximal rate of nutrient acquisition by diffusion^{10,11}. Apparently, a *Synechococcus* cell can accumulate P_i faster than either a *Prochlorococcus* or a SAR11 cell. To understand why the abundance of *Synechococcus* in the central gyre waters is three orders of magnitude lower than the abundance of *Prochlorococcus* and SAR11, we need to take into account cell sizes and cellular P requirements of these bacteria.

Once their maximal P_i clearance rates are normalized to cellular biovolumes (Supplementary Table 1 and Fig. 2a) then a *Prochlorococcus*, a *Synechococcus* or a SAR11 cell can theoretically clear all dissolved P_i from seawater $\leq 2.5 \times 10^4$, 2.6×10^4 or 1.2×10^5 times its cellular volume min⁻¹, respectively. In agreement with the surface area-to-volume concept²⁹, these biovolume-specific clearance rates show that a SAR11 cell is noticeably (4–5×) more effective in uptake of P_i than either a *Prochlorococcus* cell or a *Synechococcus* cell probably owing to the 2× higher surface area-to-volume ratio of a small, curved-rod shape SAR11 cell compared with the cocci cyanobacteria (Supplementary Fig. 3 and Supplementary Table 1).

To account for the cellular P requirements of oceanic bacterial cells, we determined their cellular P content. The cellular P content of a *Synechococcus* cell (1.93×10^7 P atoms cell⁻¹) and hence their P demand is 5–7× higher than the P content of a *Prochlorococcus* and a SAR11 cell (4.14 and 2.68×10^6 P atoms cell⁻¹, respectively, Fig. 2b and Supplementary Table 3). This implies that *Synechococcus* growth in P_i -depleted waters is constrained by its high P demand rather than by its ability to acquire P_i . It is also notable that a larger *Synechococcus* and a smaller *Prochlorococcus* have similar biovolume-specific P_i clearance rates, despite the 1.2× higher cell surface-to-volume ratio of the latter (Supplementary Table 1). As porin-restricted diffusion constrains the P_i clearance rate, the OM of *Synechococcus* ought to be more permeable to P_i , e.g., to have more P_i -specific porins per μm^2 of the OM surface.

The above comparisons show that despite its high P demand, a *Synechococcus* cell is a good model system for studying the process of P_i acquisition by oceanic bacteria. In our laboratory studies, we focused on the oligotrophic *Synechococcus* sp. strain WH8102 but also made comparisons with the mesotrophic *Synechococcus* strains WH8109 and WH7803³⁰. The 40–90× lower P_i clearance rate of larger cells of cultured *Synechococcus*

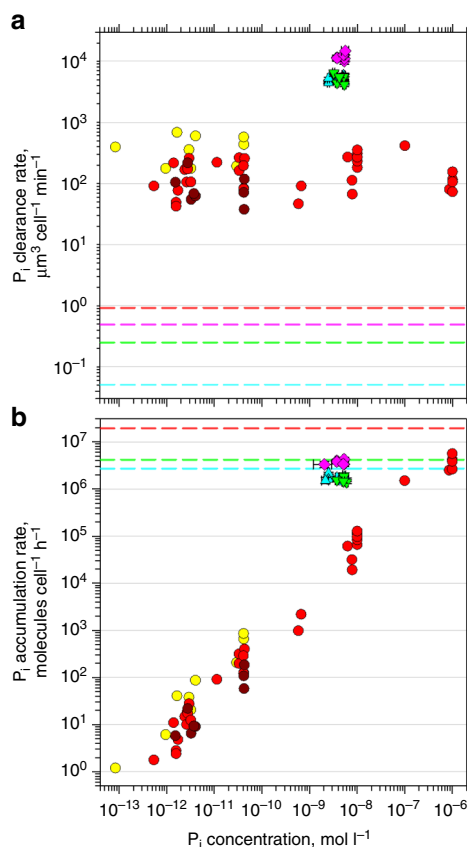


Fig. 2 P_i acquisition rates of oceanic and cultured cells. **a** Comparison of cellular P_i clearance rates of oceanic SAR11 (light blue triangles, $n = 14$), *Prochlorococcus* (green triangles, $n = 11$) and *Synechococcus* (pink diamonds, $n = 7$) at ambient P_i concentrations with rates of cultured *Synechococcus* strains WH7803 (yellow circles, $n = 10$), WH8102 (red circles, $n = 35$) and WH8109 (brown circles, $n = 8$) across a wide range of P_i concentrations. **b** Comparison of maximal cellular P_i accumulation rates of the same bacteria (SAR11 $n = 12$, *Prochlorococcus* $n = 7$, *Synechococcus* $n = 7$, WH7803 $n = 10$, WH8102 $n = 35$ and WH8109 $n = 8$). Dashed lines indicate corresponding **(a)** cellular volumes ($\mu\text{m}^3 \text{cell}^{-1}$) and **(b)** cellular phosphorus content (P atoms cell^{-1}) of oceanic SAR11 (light blue), *Prochlorococcus* (green), *Synechococcus* (pink) and cultured *Synechococcus* sp. WH8102 (orange). Horizontal grey lines indicate major ticks of the logarithmic Y-axis to assist comparing values. Symbols present individual measurements for cultured *Synechococcus* cells and mean values of four sorting replicates for oceanic bacteria; error bars indicate corresponding SD. The full range of rates of oceanic bacteria is shown in Supplementary Fig. 2. Source data are provided as a Source Data file.

compared with oceanic bacterioplankton suggests that *Synechococcus* cells grown at a P_i concentration $>10^{-5} \text{ mol l}^{-1}$ have fewer porins^{12,13} than oceanic bacteria even when the P_i concentration is downshifted (Fig. 2a). Such porin-restricted diffusion explains why a cultured *Synechococcus* cell cleared P_i from about the same volume of water, while the P_i concentration ranged over more than seven orders of magnitude. The P_i clearance rate of cultured *Synechococcus* cells remained relatively constant between the three strains down to the low end of the tested P_i concentrations (Fig. 2a), such that within a few hours these cells removed virtually all $^{33}\text{P}_i$ or $^{32}\text{P}_i$ tracers from the medium (Supplementary Table 4). Using carrier-free $^{32}\text{P}_i$ tracer, we determined that the final P_i concentration in the surrounding seawater was depleted by *Synechococcus* to $10^{-15} \text{ mol l}^{-1}$ (the instrument detection

limit), or six orders of magnitude below oceanic P_i levels (Supplementary Table 2).

Fast growth-decoupled accumulation of P_i . The rate of P_i accumulation (the amount of P_i molecules accumulated by a cell per unit of time) by cultured *Synechococcus* cells was proportional to the P_i concentration over a range of concentrations from 10^{-13} to $10^{-6} \text{ mol l}^{-1}$ (Fig. 2b), much wider than the range of 10^{-9} – $10^{-8} \text{ mol l}^{-1}$ offered by the P_i -depleted North Atlantic (Supplementary Table 2). At P_i concentrations similar to P_i -depleted oceanic waters, cultured cells accumulated P_i orders of magnitude slower than oceanic SAR11, *Prochlorococcus* and *Synechococcus* cells (Fig. 2b and Supplementary Fig. 2b). At $10^{-6} \text{ mol l}^{-1}$, a cultured *Synechococcus* cell can, however, double its cellular P content within merely 3 h (Fig. 2b and Supplementary Table 3), while they divide once every 1–2 days. Similarly, when related to their cellular P content, oceanic *Prochlorococcus* and SAR11 cells obtained sufficient P_i for cell division in merely 1–2 h, whereas in such oligotrophic waters *Prochlorococcus* divide only once every 3.5 days³¹ and SAR11 once every 2–3 days (calculated based on their cellular leucine uptake rates³²). This decoupling of P_i accumulation and growth rates in *Synechococcus*, *Prochlorococcus* and SAR11 cells suggests that, apart from being a reserve for steady growth, the accumulated P_i could have an additional, important cellular function.

***Synechococcus* cells accumulate P_i extracellularly.** To assess whether cultured *Synechococcus* cells accumulate P_i in the extracellular buffer, the accumulation of the $^{33}\text{P}_i$ -pulse and $^{32}\text{P}_i$ -chase was determined in live WH8102 cells (total P_i , Fig. 1a) and in their cellular macromolecules (biomass fixed with paraformaldehyde (PFA) that immobilizes DNA and RNA—the two principal P_i -containing macromolecules—as well as some periplasmic constituents, including PstS subunits) (Fig. 1d). After addition of the $10^{-6} \text{ mol l}^{-1}$ $^{32}\text{P}_i$ -chase, accumulation of the $^{33}\text{P}_i$ -pulse into cellular macromolecules should be halted, because any of the $4.5\text{--}7 \times 10^{-9} \text{ mol l}^{-1}$ $^{33}\text{P}_i$ -pulse that remains in the seawater would be diluted with the chase $>100\times$. However, similar to that observed in oceanic bacteria²², the pulsed $^{33}\text{P}_i$ continued to be assimilated into cell macromolecules at an unchanged rate, which started slowing down only after 5 h (Fig. 3a, c). Usually in pulse-chase experiments, incorporation of a pulsed molecule (e.g., amino acid or nucleoside) into bacterial macromolecules halts abruptly upon dilution with the chase, because the intermediate cellular labile pool of the pulsed molecule is small, e.g., 5% of the tracer incorporated into macromolecules³³. In the case of P_i , that labile pool was $10\times$ – $20\times$ larger than the amount assimilated into cellular macromolecules (Fig. 3b, d at the 3 h time point).

We then used the difference in *P_i label between the total P_i in live cells and macromolecule-bound P_i to estimate the amount of labile P_i in three *Synechococcus* strains. This showed the total *P_i content of tested live cells (Fig. 4a) to be consistently several times higher than the *P_i content of cellular macromolecules (fixed with either PFA or trichloroacetic acid (TCA), Fig. 1d,e and Supplementary Fig. 4). Furthermore, in the *P_i pre-labelled cells, which were washed and suspended in ASW with no *P_i (see Methods), the *P_i content in macromolecules increased with time and approached the total *P_i that remained stable (Fig. 4b). With no *P_i in the medium, the additional *P_i gained by the macromolecules can only be sourced from *P_i accumulated in the intermediate buffer. These data also show that the accumulated *P_i is semi-labile and can be imported into the cytoplasm to synthesize nucleic acids.

To confirm the extracellular (i.e., not in the cytoplasm) location of the labile P_i , we washed cells for 1–2 min with deionized water

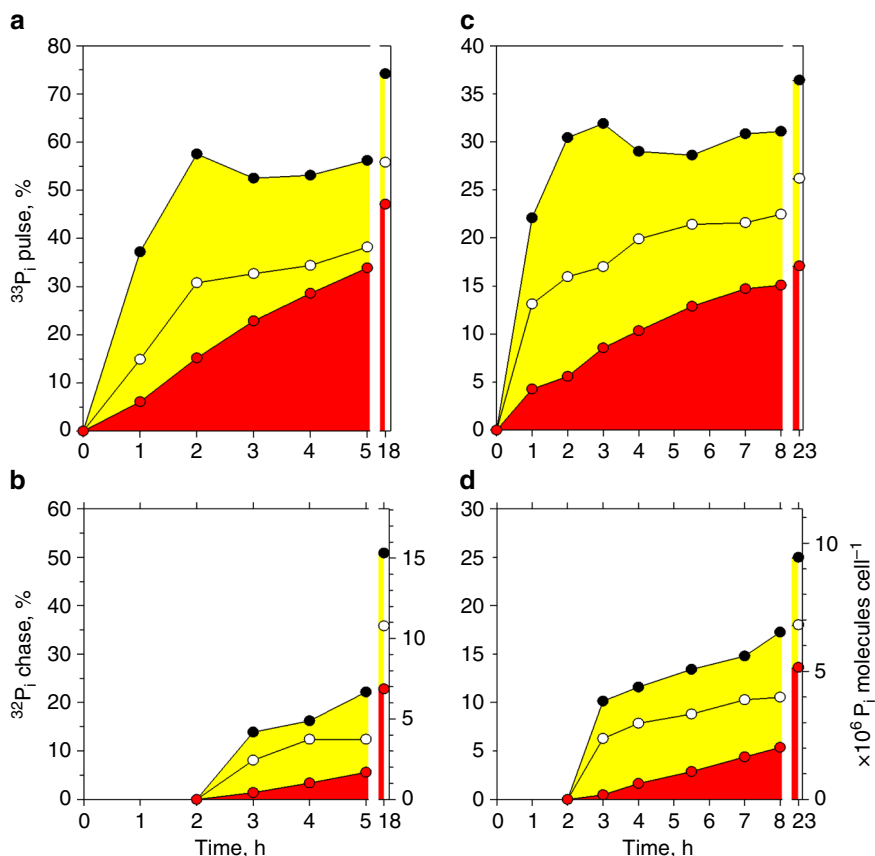


Fig. 3 P_i accumulation by *Synechococcus* sp. WH8102. Left (a, b) and right (c, d) panels show the results of two representative pulse-chase experiments with cells at exponential and early stationary growth phases, respectively. **a, c** Accumulation dynamics of 10^{-8} mol l $^{-1}$ $^{33}P_i$ -pulse added at 0 h in live cells washed with artificial seawater – the total P_i (black circles), live cells washed with deionized water – the cytoplasmic P_i (white circles) and in the PFA-fixed cellular biomass – the macromolecule-bound P_i (red circles), as a percentage of added tracer. **b, d** Accumulation dynamics of the 10^{-6} mol l $^{-1}$ $^{32}P_i$ -chase added at 2 h as the total P_i , the cytoplasmic P_i and the macromolecule-bound P_i . The additional right Y-axis (b, d) shows cellular rates of $^{32}P_i$ -chase accumulation. To assist comparison of the labile and non-labile P_i , the areas below lines are coloured yellow for the labile P_i and red for non-labile P_i . Symbols are connected with lines to indicate the slopes of the $^{33}P_i$ and $^{32}P_i$ tracer accumulation. The X-axis is broken to add an additional, final time point. Circles present mean values of technical duplicates or individual measurements. Source data are provided as a Source Data file.

(DW). Washing live cells with DW effectively strips P_i and other ions adsorbed to the OM components. In addition, such brief hypo-osmotic shock also releases the content of the periplasm without disrupting the plasma membrane. Western blotting analysis confirmed the presence of the periplasmic P_i -binding subunits PstS in the DW-washed fraction but detected no Rubisco, arguably the most abundant soluble protein in the cyanobacterial cytoplasm (Fig. 5a, b). In fact, even a 30 min incubation of *Synechococcus* in DW did not lyse the cells (Fig. 5c). As a substantial fraction of the accumulated *P_i was removed with a brief rinse of live *Synechococcus* with DW (Fig. 3), we therefore conclude that their cells accumulate P_i outside the plasma membrane, i.e., on the surface of the OM or in the periplasm (Fig. 1a†).

Periplasmic location and retention of the P_i in *Synechococcus*.

To identify the exact location of the accumulated P_i and to assess whether P_i was associated with specific cell surface ligands, we examined the response of live *P_i pre-labelled *Synechococcus* cells to a variety of treatments, which are inapplicable to delicate oceanic bacteria (Fig. 1b, c and Supplementary Tables 5 and 6). Treatments with surfactants released no *P_i (Fig. 6), suggesting that it is not associated directly with OM lipids. High concentrations of a broad-spectrum protease Proteinase K, which was

shown to efficiently digest extracellular proteins in bacteria^{34,35}, did not release the accumulated *P_i , implying no direct involvement of extracellular proteins (including the S-layer proteins of WH8102³⁶) in P_i accumulation (Fig. 6). Release of the accumulated P_i did not happen after destabilization of the spatial conformation of lipopolysaccharides (LPS) by depletion of Ca^{2+} and Mg^{2+} di-cations³⁷ (ASW- P_i -Ca and NaCl + EDTA) or by lysozyme treatment³⁸ (Fig. 6), suggesting no direct involvement of LPS in P_i accumulation. Retention of P_i by phosphorylation of extracellular macromolecules was ruled out, because alkaline phosphatase had no effect on the accumulated P_i (Fig. 6). Incubations with either acidic (pH 6) or alkaline (pH 10) ASW failed to remove the accumulated P_i (Fig. 6), demonstrating an insignificant effect of (de)protonation on the stability of the accumulated P_i .

To assess the role of PMF in retention of the accumulated P_i , we treated *P_i pre-labelled *Synechococcus* cells with the inhibitor carbonyl cyanide m-chloro-phenyl-hydrazone (CCCP) (Supplementary Table 7). Dissipation of the PMF had a minor effect on the already accumulated P_i : the amount of released P_i was comparable to the amount of P_i lost by washing live cells with ASW- P_i (Supplementary Fig. 4). In contrast to the above treatments, accumulated P_i was easily removed by short (1–2 min) rinses of live cells with a range of hypotonic solutions

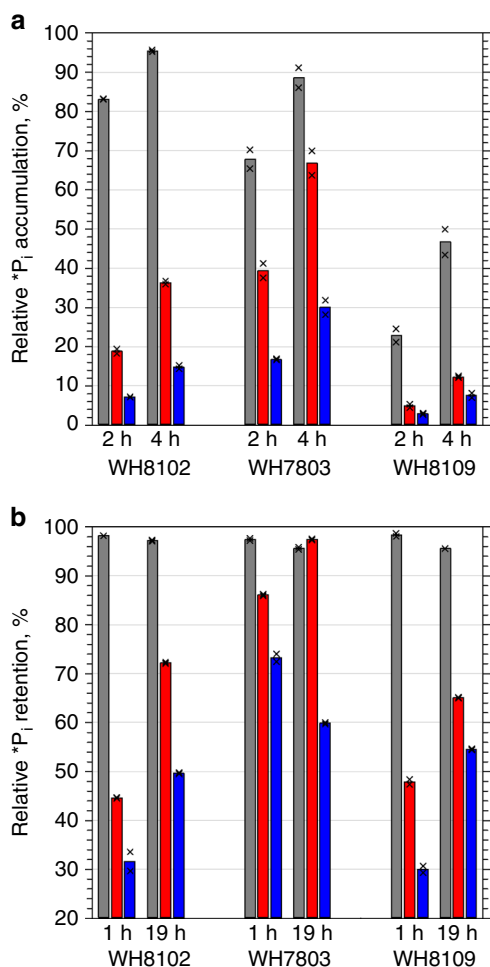
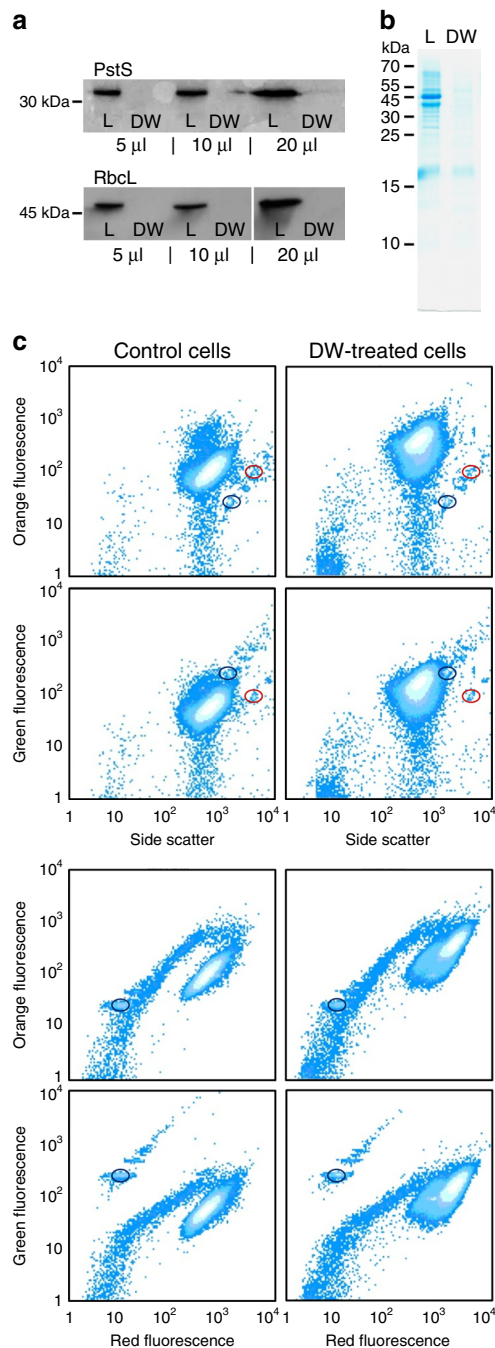


Fig. 4 Accumulation and retention of the accumulated $^{32}\text{P}_i$ by *Synechococcus*. **a** The total P_i accumulated in live cells (grey bars) compared with the amount of P_i in PFA-fixed cellular macromolecules (red bars) and TCA-precipitated nucleic acids (blue bars). Cells washed to remove the free P_i were re-suspended in ASW- P_i , supplemented with 100 Bq ml^{-1} of $\text{H}_3^{32}\text{PO}_4$, incubated under standard cultivation conditions and sampled after 2 and 4 h. **b** Retention of the total accumulated P_i in $^{32}\text{P}_i$ pre-labelled cells and its internalization into macromolecules and nucleic acids. The pre-labelled cells re-suspended in ASW- P_i were incubated under standard cultivation conditions and sampled after 1 and 19 h. The plots show the results of representative experiments. Bars present mean values of technical duplicates indicated as crosses. Horizontal grey lines indicate major ticks of the Y-axis to assist comparing values. Source data are provided as a Source Data file.

(Fig. 7), i.e., ASW diluted 1:10–1:100, phosphate-buffered saline or DW (Supplementary Table 8), which release periplasmic cell contents^{27,39} but do not cause osmotic cell lysis of marine *Synechococcus* (Fig. 5). Hypotonic washes reproducibly removed an amount of $^{32}\text{P}_i$ less than, or similar to, that removed from the PFA-fixed cellular macromolecules (Figs. 3 and 7). Thus, resistance to a variety of extracellular treatments (Fig. 6) in conjunction with the hypotonic removal of the accumulated P_i (Figs. 3, 5 and 7) strongly indicates the periplasmic location of the accumulated P_i .

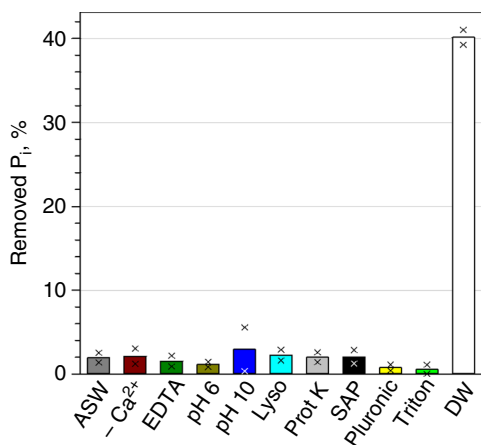
The PMF is essential for P_i accumulation. The inhibitor CCCP has previously been used to investigate the role of the PMF in various aspects of cyanobacterial physiology^{26,27}. Although we used this inhibitor to specifically elucidate the role of the PMF in



P_i accumulation by cultured *Synechococcus* cells, we compared the CCCP effect with the effect of three other metabolic inhibitors (Supplementary Table 7) on P_i acquisition by oceanic bacterioplankton to safeguard from potential artefacts. A similar time course of P_i clearance by the control and 3-(3,4-dichloro-phenyl)-1,1-dimethylurea (DCMU)-treated bacterioplankton demonstrates that DCMU (which reduces photosynthetic electron flow and proton extrusion) slows down the microbial P_i clearance rate by ~30% (Supplementary Fig. 5). This reduction is consistent with the percentage (~30%) of cyanobacterial cells within the total bacterioplankton. The other three inhibitors completely terminated P_i clearance by bacterioplankton, as no time course was observed (Supplementary Fig. 5). The effect of N,N'-dicyclohexyl-carbodiimide (DCCD, an ATPase inhibitor) was delayed three times longer compared with 2,5-dibromo-3-methyl-6-

Fig. 5 Hypotonic release of the periplasm without lysing *Synechococcus* sp. WH8102 cells.

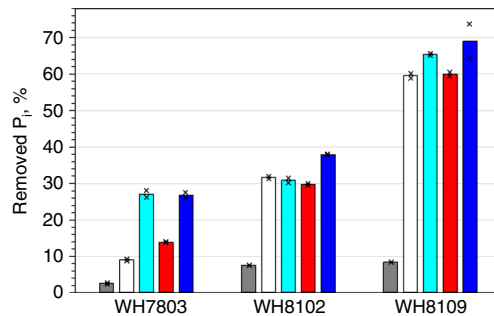
Western blotting of periplasmic and cell lysate proteins (a, b). Cells were subjected to 1 min hypotonic shock in deionized water (DW) and pelleted to separate treated cells from supernatant. Proteins present in the DW supernatant were compared with proteins in the lysate (L) of treated cells. **a** Western blot immunolabeling with antibodies against the periplasmic P_i -binding subunit PstS and the large Rubisco subunit RbcL (5, 10 or 20 μ l per lane) reveals the presence of PstS but no signal for RbcL in the DW supernatant. **b** Coomassie-stained SDS-PAGE (10 μ l per lane) with the size range of proteins in the L and DW samples is shown for reference. Mw, molecular-weight size marker (kDa). The experiment was repeated independently four times with similar results. Comparison of control (left column) and DW-treated cells (right column) using flow cytometric pseudo-colour plots (c) of cellular orange or green autofluorescence vs. red autofluorescence or side scatter. Visualized in BD CellQuest™ Pro, cellular light scatter and autofluorescence of photosynthetic pigments cluster cells in a single cytometric population separate from a dispersed cluster of other suspended particles and tight clusters of reference beads. Compared with the control cells incubated in ASW medium, the cells incubated in DW for 0.5 h have higher autofluorescence but still form a single population, which shows minor deterioration, i.e., cell lysis. Cells were analysed without fixation or staining. The yellow-green (505/515 nm) 0.5 μ m beads (circled in dark blue) and multifluorescence 1.0 μ m beads (circled in red) were used as an internal reference. Source data are provided as a Source Data file.

**Fig. 6 Retention of the accumulated P_i by live, pre-labelled *Synechococcus* sp. WH8102 cells.**

Minor removal of P_i label was achieved by the following treatments: ASW, cells washed with artificial seawater; $-Ca^{2+}$, cells washed with ASW without Ca^{2+} ; EDTA, cells washed with isotonic NaCl solution containing EDTA; pH 6 and pH 10, cells washed with ASW at pH 6 and at pH 10, respectively; Lyso and Prot K, cells incubated with lysozyme and Proteinase K, respectively for 15 min; SAP, cells incubated with shrimp alkaline phosphatase for 30 min; Pluronic and Triton, cells incubated with the surfactants Pluronic F-68 and Triton X-100, respectively, for 15 min. A short wash with deionized water (DW) removed about 40% of the P_i label. The plot summarizes the results of the representative experiments. Bars present mean values of technical duplicates indicated as crosses. Horizontal grey lines indicate major ticks of the Y-axis to assist comparisons. For details, refer to Supplementary Tables 5 and 6. Source data are provided as a Source Data file.

isopropylbenzo-quinone (DBMIB) and CCCP, which halted P_i accumulation after 4 min (Fig. 8a, grey bars).

Likewise, CCCP was a highly effective inhibitor of P_i accumulation by cultured *Synechococcus* cells (Fig. 8a). The time delay of 3–5 min common to the three strains was similar to the 4

**Fig. 7 Osmotic removal of the accumulated P_i from the P_i pre-labelled cells.**

Comparison of removable P_i from live cells of the three *Synechococcus* strains incubated for 1 h and washed with artificial seawater (grey bars), deionized water (white bars) and phosphate-buffered saline (turquoise bars) vs. PFA-fixed cellular macromolecules (red bars) and TCA-precipitated nucleic acids (blue bars). The plot shows the results of a representative experiment. Bars present mean values of technical duplicates indicated as crosses. Horizontal grey lines indicate major ticks of the Y-axis to assist comparisons. Source data are provided as a Source Data file.

min delay of CCCP-treated bacterioplankton. This abrupt halt of P_i accumulation by CCCP-treated *Synechococcus* cells indicates that, as in experiments with bacterioplankton (Fig. 8a), membrane depolarization rather than ATP depletion is behind the inhibition, whereas the generic 4 min delay presumably reflects the time required for CCCP molecules to integrate into cellular membranes. As there was <1 min to incorporate P_i into the PFA-fixed macromolecules and even less time to incorporate it into TCA-fixed nucleic acids (Fig. 1d, e), the bulk of the accumulated P_i in CCCP-treated cells (32% and 11% of the total P_i was in the PFA-fixed macromolecules of oceanic bacteria and isolates, respectively) remained labile (Fig. 8a). This comparison of live and fixed cells worked equally well for bacterioplankton and for cultures (Fig. 8a), confirming that in all bacteria tested P_i is first accumulated in the periplasm before being imported into the cytoplasm and assimilated.

The PMF consists of the transmembrane chemical H^+ gradient (ΔpH) and the transmembrane electric gradient ($\Delta\Psi$) that can be sustained by other cations. The protonophore CCCP dissipates both the ΔpH and $\Delta\Psi$. To specifically link one of the components to P_i accumulation in the periplasm, we abolished $\Delta\Psi$ in WH8102 using the three cation-specific ionophores: a K^+ -specific ionophore (Valinomycin), a monovalent cation-specific (e.g., Na^+ and K^+) ionophore (Monensin) and a divalent metal-specific (e.g., Mn^{2+} , Ca^{2+} and Mg^{2+}) ionophore (A23187, Supplementary Table 7), which facilitate the electroneutral transport of cations through a membrane down the chemical gradient. Compared with the control, the three ionophores reduced P_i accumulation into live cells by 0.4 \times , 1.5 \times and 2.6 \times , respectively (Fig. 8b). A significant fraction (20–37%) of the accumulated P_i remained in the periplasm. As relative to the protonophore CCCP, the three ionophores had a minor effect on P_i accumulation by *Synechococcus* cells (Fig. 8b), we conclude that ΔpH rather than $\Delta\Psi$ is crucial for the periplasmic P_i accumulation. To validate conclusions about energy-dependent accumulation of P_i , drawn from the inhibitor-based experiments, we tested whether P_i accumulation by SAR11, *Prochlorococcus* and *Synechococcus* cells could be energy-stimulated. Conveniently, these bacteria use light energy in their metabolism.

Light stimulation of P_i accumulation. To test whether light can energize bacterial P_i accumulation, we compared P_i clearance by oceanic bacterioplankton cells incubated in the light vs. dark

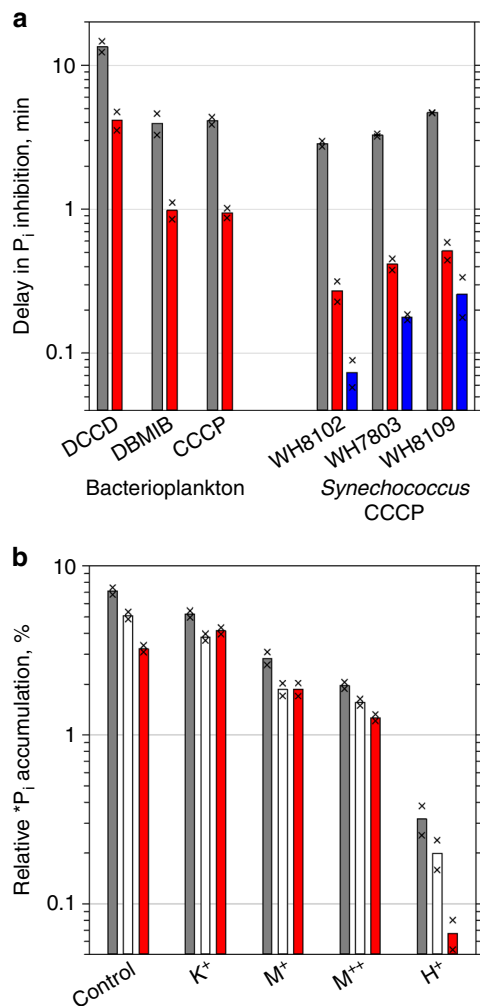


Fig. 8 Inhibition of bacterial P_i accumulation. **a** Comparison of the time delay in the inhibition of *P_i accumulation between bacterioplankton treated with DCCD, DBMIB and CCCP, and *Synechococcus* strains WH8102, WH7803 and WH8109 treated with CCCP. The time delay is derived from the rate of P_i accumulation, measured for uninhibited control cells. **b** Relative P_i accumulation in *Synechococcus* sp. WH8102 cells treated with the K^+ -specific ionophore Valinomycin (K^+), the monovalent metal-specific ionophore Monensin (M^+), the divalent metal-specific ionophore A23187 (M^{++}) and the protonophore CCCP (H^+). Plots show the results of representative experiments. Bars present mean values of technical duplicates indicated as crosses. Horizontal grey lines indicate major ticks of the logarithmic Y-axis to assist comparing values for the following treatments: P_i accumulation into live cells washed with seawater (grey bars), into PFA-fixed cellular macromolecules (red bars) and into TCA-fixed cellular nucleic acids (blue bars) (**a**) or into the cytoplasm (white bars) of cells washed with deionized water (**b**). Source data are provided as a Source Data file.

(Fig. 9). Indeed, light enhanced P_i accumulation by all cells studied (Supplementary Table 9). Compared with spectacular (≤ 10 times) but sporadic light stimulation of P_i clearance by *Prochlorococcus* cells (and to a lesser extent by *Synechococcus* cells), light stimulation of P_i clearance by SAR11 cells was more uniform, averaging 40% (Fig. 9). Counter-intuitively, light stimulation was distinctly more pronounced at lower rates of P_i clearance in moderately P_i -depleted waters bordering the North Atlantic subtropical gyre but absent at the maximal rates of P_i clearance in the P_i -depleted gyre (Fig. 9 and Supplementary Table 2).

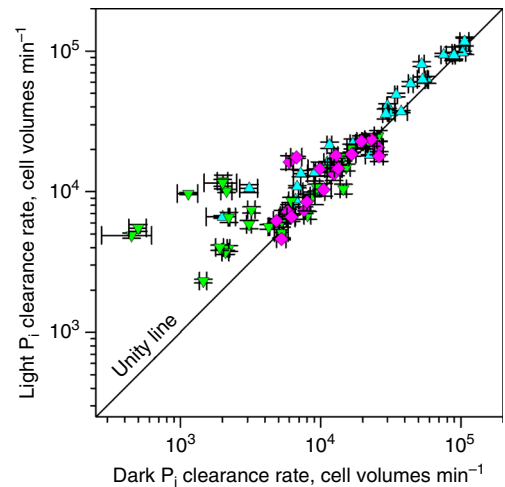


Fig. 9 Comparison of P_i clearance rates of oceanic cells in the light versus dark. Comparison of P_i clearance rates in cell volume equivalents of oceanic SAR11 (turquoise triangles, $n = 28$), *Prochlorococcus* (green triangles, $n = 32$) and *Synechococcus* (pink diamonds, $n = 19$) at ambient P_i concentrations. Equivalents of cell volumes cleared of P_i per minute were used to negate the bacterial size differences. Symbols present mean values of four sorting replicates of the paired light vs. dark experiments; error bars indicate corresponding SD. Source data are provided as a Source Data file. Values above the unity line indicate light stimulation.

Discussion

Accumulation of P_i in the periplasm starts with P_i diffusion from seawater. The theoretical maximal rate of P_i diffusion into the periplasm of a Gram-negative cell depends on a P_i diffusion coefficient and the permeable surface area^{10,11}. The P_i diffusion coefficient is a seawater trait affecting all cells equally. Cells could, however, control their P_i -permeable surface area by varying the number of OM porins. *Prochlorococcus* and *Synechococcus* strains respond to P_i limitation by the increased expression of P_i -specific porin genes and the increased abundance of porin proteins^{14,40,41}. However, the number of these porins in the OM cannot increase indefinitely. Indeed, the maximal P_i clearance rates of oceanic cyanobacterial and SAR11 cells (Fig. 2a) converge towards $\sim 30\times$ below the theoretical maximum. The apparent upper limit to the number of P_i -specific OM porins is probably a result of the competition for space between porins selective for different small solutes, acquisition of which is essential for a living cell.

In contrast to other solutes, P_i somehow accumulates in the periplasm. *Synechococcus* cells rapidly accumulate labile P_i , which is then steadily internalized and assimilated into macromolecules (Figs. 3 and 4). The semi-labile nature of the accumulated P_i (hypotonic removal, Figs. 1c, 3 and 5–7) in conjunction with its resistance to a variety of extracellular treatments (Fig. 6) points to its periplasmic location. Diffusion-driven P_i acquisition¹¹ can deplete environmental P_i concentrations at a constant clearance rate down to $10^{-12} \text{ mol l}^{-1}$ (Fig. 2a). This is feasible only if the periplasmic P_i concentration of *Synechococcus* cells is $< 10^{-12} \text{ mol l}^{-1}$. Even if we assume that the affinity of the *Synechococcus* PstS subunit for P_i is sufficient to bind P_i at $< 10^{-12} \text{ mol l}^{-1}$ concentrations (five orders of magnitude below the determined affinity²⁰) then every P_i molecule that enters and stays in the *Synechococcus* periplasm needs to be instantly bound by a PstS subunit (Fig. 1a†). Sequestration of 6.7×10^6 molecules (Fig. 2b) of labile P_i in the periplasm would require an equal number of PstS subunits. The volume of a PstS subunit of $3.5 \times 4 \times 7 \text{ nm}$ dimensions⁴² is $\sim 5.1 \times 10^{-23} \text{ l}$, whereas the periplasmic volume of *Synechococcus* is

$\sim 2 \times 10^{-17}$ l. This is sufficient to accommodate merely 4×10^5 PstS subunits, or $17\times$ less than the number required. However, even if 4×10^5 PstS subunits cram into the periplasm, there would be no room left for other known periplasmic constituents: substrate binding subunits of at least some of 41 other ABC-type transporters in WH8102⁴³, periplasmic enzymes, e.g., alkaline phosphatase^{6,44} and aminopeptidase⁴⁵, and peptidoglycan gel matrix—the major structural component of periplasm⁴⁶. As *Prochlorococcus* cells that have a smaller periplasm⁴⁷ can have as many ABC-type transporters and periplasmic enzymes as WH8102⁴³ but accumulate more P_i in their buffer (1.2×10^7 molecules²²), it makes it even less probable that all periplasmic P_i is bound by PstS subunits. Finally, up to $20\times$ more P_i (e.g., at the 3 h time point in Fig. 3b, d, yellow) remains labile in living *Synechococcus* cells than is incorporated into bacterial macromolecules (which should include PFA-cross-linked PstS subunits, Fig. 1d). As the PstS-mediated P_i uptake model (Fig. 1a†) cannot explain the results of our experiments, an alternative explanation is required.

The evident capacity of *Synechococcus* to import the accumulated P_i into the cytoplasm (Figs. 3 and 4b) is inconsistent with passive sorption of P_i to the outer cell surface^{48,49}, because passively adsorbed P_i cannot effectively diffuse into the periplasm (Fig. 1a†). Passive sorption of P_i by marine bacteria is furthermore questionable, because metabolically inactive but structurally intact bacterioplankton cells (e.g., CCCP-, DBMIB-, DCCD-incapacitated cells) should retain their capacity to adsorb P_i passively, but instead, they do not adsorb *P_i present in seawater for hours (Supplementary Fig. 5). In contrast, the rapid cessation or slowing down of P_i accumulation caused by the specific inhibitors (Fig. 8) and light stimulation of P_i accumulation (Fig. 9) indicates that P_i accumulation in the periplasm is a metabolically active process.

Light could enhance P_i accumulation by SAR11 cells through a proteorhodopsin-generated PMF⁵⁰. Cyanobacteria could use photosynthetically generated PMF for the same purpose. The former energy generator consistently increased P_i accumulation by 40%, whereas the latter energy generator showed a higher ($\leq 10\times$) potential to boost P_i accumulation by *Prochlorococcus* cells (Fig. 9). Although such considerable light stimulation is notable, the most unexpected result of the light vs. dark experiments was the lack of light stimulation at the higher rates of P_i accumulation (Fig. 9) in the P_i -depleted waters of the North Atlantic subtropical gyre²². Apparently, under severe P_i depletion, bacteria do not rely on light as the primary energy source for P_i acquisition but use their internal energy sources. P_i accumulation seems so important for bacteria that their maximal P_i clearance rates ($\sim 30\times$ below the theoretical maximal rate of nutrient acquisition by diffusion) are probably constrained by the limited OM surface for incorporating P_i -specific porins rather than by the availability of cellular energy.

It seems inexplicable that bacteria can accumulate millions of P_i molecules (Figs. 2b and 3b, d, and Supplementary Fig. 2b) in their periplasm, while maintaining diffusion even at exceedingly low environmental concentrations. The high percentage of *P_i present in the periplasm (Figs. 4–7) and the gradual assimilation of accumulated P_i (Figs. 3–4) indicates that the rate of periplasmic P_i accumulation by far exceeds the rate of P_i import. The parallel import of $^{33}P_i$ pulse and $^{32}P_i$ chase (Fig. 3) means that the spatial distribution of P_i in the periplasm is not ordered. Bacteria do not synthesize polyphosphates in the periplasm but somehow make P_i molecules semi-labile: accessible for PstS subunits but prevented from diffusing back into seawater. On the one hand, periplasmic P_i needs to remain in ionic form rather than phosphorylate organic molecules, because PstS subunits specifically bind HPO_4^{2-} and $H_2PO_4^-$ ions⁴². On the other hand, P_i cannot be maintained as free ions because a few free P_i ions would make

the periplasmic concentration of P_i above the environmental concentration and hence reverse diffusion. The nearly instantaneous termination of P_i accumulation (Fig. 8a) by the inhibitors CCCP and DBMIB (which dissipate the PMF and thereby halt ATP generation), compared with the delayed reduction of P_i accumulation by DCCD (which primarily blocks ATP generation and thus destroys ATP-sustained membrane potential), strongly indicates that P_i accumulation is linked to cellular energetics through the PFM rather than being directly driven by ATP through PstSCAB-type transporters (Fig. 1a†). The mutually exclusive conditions (listed above) of PMF-dependent P_i accumulation in the periplasm cannot be explained by PstS-mediated P_i import (Fig. 1a†). Therefore, an alternative mechanism is needed.

An alternative mechanism of PMF-dependent P_i accumulation in the periplasm is a conjecture, because we know little about the organization and functioning of the periplasm⁴⁶ in a living bacterial cell. A cell maintains the PMF by extruding protons (H^+ ions) across the plasma membrane against the electrochemical gradient using the energy of respiration and photosynthesis^{50–52}. Accumulation of H^+ in the periplasm would make it acidic relative to both the cytoplasm (pH ~ 7.2 ⁵³) and seawater (pH 8.0–8.3⁵⁴) (Fig. 1a†). However, it is unlikely that many free H^+ ions would accumulate in the periplasm of marine bacteria, because their OM is permeable to the smallest H^+ ions. Hence, H^+ ions should diffuse out into the environment to be neutralized by $>100\times$ excess of OH^- ions in alkaline (pH 8.0–8.3) seawater⁵⁴, thereby dissipating the membrane potential. To prevent the dissipation of the H^+ -based gradient, H^+/Na^+ antiporters may exchange at least some of the periplasmic H^+ ions for Na^+ ions⁵⁵. This substitution could preserve the electrical gradient and support ATP production through H^+ -ATP synthases, which can transport Na^+ ⁵⁶. Genes for both the H^+/Na^+ antiporter and the Na^+ -driven ATP synthase are present in genomes of *Prochlorococcus*⁵⁶ and *Synechococcus* isolates (e.g., NP_875999⁵⁶, WP_010315318, WP_025922676, WP_002805629 and WP_062436653).

The electric potential between the acidic positively charged periplasm and the alkaline seawater would facilitate diffusion, or more precisely mass transfer, of anions with higher negative charge more strongly than anions with lower negative charge. Thereby, mass transfer through anion-selective porins¹³ of HPO_4^{2-} and PO_4^{3-} anions (which comprise 29% and 0.01% of the total P_i in seawater at pH 8.0, respectively^{57,58}) would be particularly favourable. Stronger cationic association of the main seawater anions (e.g., Cl^- , HSO_4^- , HCO_3^- and NO_3^-) would also favour mass transfer of free P_i anions. Once in the H^+ -enriched periplasm, the HPO_4^{2-} and PO_4^{3-} anions would associate with one or two H^+ and metal cations to reach pH-dependent speciation equilibrium^{57,58}. Kinetic stability of neutral P_i molecules would explain why disruption of the membrane potential only has a minor immediate effect on the P_i already accumulated in the periplasm (Supplementary Fig. 4).

Neutralization of cations with P_i anions would reduce the PMF, but that could be restored via continuous extrusion of H^+ and cations across the plasma membrane to maintain mass transfer of P_i anions through porins as long as free P_i anions can mass transfer from the environment (Fig. 1a†). Mass transfer would stop when equilibrium is reached, i.e., all P_i anions remaining in seawater are too strongly associated with environmental cations and molecules of water. The strength of their association depends on the total ionic composition of environmental solutions⁵⁸; in seawater, the association of P_i anions is apparently weak, because we observed bacterial accumulation of P_i anions to continue down to environmental concentrations $<10^{-12}$ mol l⁻¹ (Fig. 2) and even $<10^{-15}$ mol l⁻¹ (Supplementary Table 4).

Although the periplasm becomes saturated with P_i in 1 h (e.g., 4×10^6 P_i molecules in 2.1×10^{-17} l periplasm equals 0.3 mol l^{-1} , Fig. 3b, d), a cell somehow averts precipitation of the P_i salts in the periplasm. To prevent formation of insoluble P_i salts, a cell would need to minimize concentrations of divalent cations (e.g., Ca^{2+} and Mg^{2+} , which associate with P_i to form salts with low solubility) in the periplasm, while balancing the concentrations of monovalent cations (e.g., Na^+ and K^+) and P_i anions to form neutral soluble ion pairs in a way analogous to the common phosphate buffer. Although cation-associated, the H_2PO_4^- and HPO_4^{2-} ions remain accessible to PstS-mediated (the PstS subunits have specific affinity to these two anion forms⁴²) import, because they remain soluble (Fig. 1a†). Formation of neutral ion pairs would maintain mass transfer of HPO_4^{2-} and PO_4^{3-} into the periplasm, and prevent H^+ from escaping into seawater. To simplify the explanations we give below, we suggest to term this periplasmic H^+ -driven phosphate-cation association—phosphatation.

Maintaining maximal rates of P_i acquisition irrespective of the availability of light energy (Fig. 9) suggests that periplasmic phosphatation is functionally important for marine bacteria as different as cyanobacteria and SAR11 alphaproteobacteria. We propose the following three physiological functions of periplasmic phosphatation: (i) The periplasmic association of P_i with chemiosmotic cations accumulates not only P_i , but also cations. Accumulation of the latter could be viewed as energy conservation, because H^+/Na^+ import through the plasma membrane can generate ATP^{59,60}. (ii) The high concentration of P_i accumulated in the periplasm could also ensure that the PstS transport system is always saturated with P_i and operates near its maximal rate. (iii) Periplasmic phosphatation could have an osmotic function. The concentration of P_i in the periplasm can increase by 0.3 mol l^{-1} in just 1 h (e.g., 4×10^6 P_i molecules in 2.1×10^{-17} l periplasm, Fig. 3b, d) and reach $>0.5 \text{ mol l}^{-1}$ within 3 h. Accumulation of an additional 0.5 mol l^{-1} of P_i salt would increase periplasmic osmolarity by $\sim 0.5 \text{ osmol l}^{-1}$. Considering that there are other osmotically active molecules in the periplasm, and that the P_i salt concentration could raise further the periplasmic osmolarity, this would easily exceed the osmolarity of seawater, i.e., $\sim 1 \text{ osmol l}^{-1}$ ⁵⁷. To equilibrate, the resultant osmotic differential water molecules would enter the periplasm increasing its volume and the OM turgor (Fig. 1a†), explaining how the OM could work as a load-bearing element⁶¹. Therefore, we predict that periplasmic phosphatation is essential for bacterial osmotic regulation—a hypothesis worth testing experimentally.

There is little doubt that the cationic attraction of P_i anions predates life. It was proposed that back in the earliest Archean, positively charged clay particles in oceanic cold alkaline seeps could be viewed as primordial membranes of protocells⁶². Their positive charge would similarly attract P_i anions from seawater and this initial enrichment of clay particles with P_i might have been inherited by the first living forms, who gradually engaged P_i in cellular energetics and later genetics. Thus, periplasmic phosphatation is inherently essential for bacterial cells, because it could conserve energy as well as store and attract the vital P_i .

Methods

Environmental sampling. Data were collected on five oceanographic cruises (Supplementary Table 2) on board the Royal Research Ships *James Clark Ross* (JCR), *James Cook* (JC), *Discovery III* (D) and *Discovery IV* (DY), and the Research Vessel *Maria S. Merian* (MSM) in the North Atlantic during Atlantic Meridional Transect cruises AMT17-D299, AMT20-JC053, AMT22-JC079 and AMT27-DY084 in September–October 2005, 2010, 2012 and 2017, respectively, and during the MSM03 cruise in September–October 2006. At predawn, midday and occasional evening stations seawater samples were collected from 20 m (a representative depth from the surface mixed layer unaffected by the ship's movement and

contamination) using a 20×201 Niskin bottle rosette (Miami, FL, USA) mounted on the stainless steel frame of a conductivity-temperature-depth profiler. Samples were decanted into 101 polyethylene carboys. Experiments commenced within 1–2 h after sample collection. The concentrations of bioavailable P_i were determined using isotope dilution, concentration series bioassays^{7,22} with carrier-free ^{32}P -labelled or ^{33}P -labelled orthophosphoric acid (Hartmann Analytic GmbH, Braunschweig, Germany). Bioassay experiments were performed in polypropylene, screw cap, 2 ml micro-centrifuge tubes (Starlab, Milton Keynes, UK). Flow-sorting experiments and experiments with inhibitors were performed in Pyrex glass bottles (Fisher Scientific, Loughborough, UK). To minimize artificial contamination (e.g., P_i , other nutrients, heavy metals), all plastic-ware, glassware and silicone tubing were soaked in 10% HCl and repeatedly rinsed with DW and sampled seawater.

Synechococcus strains and growth conditions. We chose *Synechococcus* sp. WH8102, because its P_i acquisition and utilization strategies are known^{1,41}. This strain belongs to clade III that is generally considered to be adapted to low-nutrient conditions^{63,64} and abundant in P_i -depleted Atlantic waters⁶⁵. Strain *Synechococcus* sp. WH8109 is a member of clade II, a clade that dominates tropical and subtropical regions of the world's ocean^{66,67}, tolerates intermediate nutrient-depleted conditions^{64,67} and lives in nutrient-richer upwelling waters⁶⁵. It was reasonable to expect that these strains accumulate P_i extracellularly, because they grow better under P_i -depleted rather than under P_i -replete conditions³⁰. To elucidate whether the P_i accumulation was specific to cyanobacterial ecotypes that had evolved to cope with P_i deprivation, we also included an opportunistic strain *Synechococcus* sp. WH7803 (clade V) that reaches a maximal growth rate when supplemented with $\geq 10^{-6} \text{ mol l}^{-1}$ P_i ⁴⁹.

Cultures of *Synechococcus* sp. WH8102 and *Synechococcus* sp. WH7803 were axenic. An axenic culture of *Synechococcus* sp. WH8109 strain was established by flow sorting. Live bacterial cells in a mixed culture were stained with $0.1 \mu\text{g ml}^{-1}$ Hoescht 33342 (final concentration) and *Synechococcus* sp. WH8109 cells were flow cytometrically differentiated from other bacteria by their specific autofluorescence. Using a custom-built MoFlo XDP instrument⁶⁸, WH8109 cells were flow-sorted in batches of 10–200 cells directly into sterile tubes with ASW medium. Tubes were placed into an illuminated growth chamber and incubated until growth became evident by colour.

Axenic cultures of *Synechococcus* sp. strains WH8102, WH8109 and WH7803 were cultivated in an ASW medium⁷⁰ prepared using American Chemical Society grade reagents and supplemented with $8 \times 10^{-5} \text{ mol l}^{-1}$ K_2HPO_4 . Semi-continuous cultures were maintained at 23°C with gentle agitation at 100 r.p.m. on an orbital shaker at a light intensity of $\sim 20 \mu\text{mol photons m}^{-2} \text{ s}^{-1}$. Axenic cultures were monitored regularly for contamination by plating $\sim 10^6$ cells on ASW agar plates containing 0.5 g l^{-1} yeast extract and were contaminant free. To maintain trace P_i conditions, glassware used for P_i -free cultivation and experiments was soaked in 10% HCl and thoroughly rinsed with DW.

Cell enumeration and flow sorting. Cultured *Synechococcus* cells were counted live, unstained, to assess their cell integrity during laboratory experiments (e.g., see Fig. 5c). Oceanic samples were fixed with PFA (1% w/v final concentration), stained with SYBR Green I DNA dye⁶⁹ at 20°C in the dark for 1 h and flow cytometrically counted and sorted^{22,70} (Supplementary Fig. 1). Bacterioplankton cells flow-sorted during the D299 and JC053 cruises were taxonomically identified using fluorescence in situ hybridization⁷⁹. High nucleic acid-containing bacteria with virtually undetectable chlorophyll autofluorescence⁷¹ were identified as *Prochlorococcus*. Low nucleic acid-containing bacteria were identified as SAR11 alphaproteobacteria. Oceanic *Synechococcus* were identified flow cytometrically based on their specific orange autofluorescence⁷.

Western blot analyses. Cells from an exponentially growing *Synechococcus* WH8102 culture ($\text{OD}_{750} = 0.25$) were starved for P_i to induce PstS synthesis. After 60 h incubation, 800 ml cells were pelleted by centrifugation, washed twice with 20 ml ASW and subjected to 1 min hypotonic shock in 6 ml DW. Following centrifugation, supernatant (6 ml) was collected. The remaining cell pellet was suspended in 6 ml cold DW, supplemented with Protease Inhibitor Cocktail II (Abcam) and the cells were disrupted by two passes through a high-pressure Cell Disruptor (Constant Systems Ltd, Northants, UK). Intact cells were removed from hypotonic DW supernatant and disrupted cells by short centrifugation ($5000 \times g$, 10 min, 4°C). Large membrane debris of disrupted cells were removed using high-speed centrifugation ($20,000 \times g$, 60 min, 4°C) and the remaining cell lysate (6 ml) was collected. Volumes (5, 10 or 20 μl) of DW supernatant and cell lysate were denatured with 1:3 (v/v) sample buffer at 90°C for 5 min and separated by SDS-polyacrylamide gel electrophoresis using 14% acrylamide. A reference gel was stained with Coomassie blue. Western blot immunolabelling used antibodies against the periplasmic phosphate-binding subunit PstS⁷² (1:10,000 dilution) and the large Rubisco subunit RbcL (1:10,000; AS03 037, Agrisera). For western blotting, proteins were transferred to the polyvinylidene difluoride (PVDF) membrane and analysed using standard protocols, following the use of a horseradish peroxidase (HRP)-conjugated goat anti-rabbit IgG HRP-linked secondary antibody (1:5000; #7074, Cell Signaling Technology®).

Pulse-chase experiments. Exponentially growing *Synechococcus* sp. WH8102 cells ($0.3\text{--}3 \times 10^7$ cells ml^{-1}) were collected on a $0.2 \mu\text{m}$ pore size Nuclepore track-etched filter membrane (Whatman International, Ltd, Maidstone, UK) mounted in a filter holder (Swinnex, Millipore, Ireland) and washed with 40 ml P_i -free ASW (ASW- P_i) at a flow rate of 2 ml min^{-1} using a syringe pump (KD Scientific, Holliston, MA, USA). The washed cells were pulsed with $10^{-8} \text{ mol l}^{-1} \text{ P}_i$ traced with $^{33}\text{P}_i$ ($\text{H}_3^{33}\text{PO}_4$, specific activity $\sim 111 \text{ TBq mmol}^{-1}$; Hartmann Analytic GmbH, Braunschweig, Germany) for 2 h. The pulse was chased with $100 \times \text{P}_i$ concentration ($10^{-6} \text{ mol l}^{-1}$) traced with carrier-free $^{32}\text{P}_i$ ($\text{H}_3^{32}\text{PO}_4$, specific activity $\sim 222 \text{ TBq mmol}^{-1}$; Hartmann Analytic GmbH, Braunschweig, Germany) and incubated for up to 23 h. Retention of $^{33}\text{P}_i$ and $^{32}\text{P}_i$ was determined for live and PFA-fixed cells (Fig. 3). Dissolved tracer was washed from live cells with ASW- P_i using a $0.2 \mu\text{m}$ pore size PVDF membrane spin column (Proteus Mini, Geronor, Maidenhead, UK): 0.5 ml cells were placed in a column, spun down at $5000 \times g$ for 1 min and washed thrice with 0.1 ml of ASW- P_i . The radioactivity was determined separately for the cells retained in the spin column insert and for the effluent in the collection tube. To fix cells, $0.5\text{--}1.5 \text{ ml}$ cells were fixed with 1% PFA, incubated at ambient temperature for 1 h and filtered on $0.2 \mu\text{m}$ pore size polycarbonate filters. Filters were rinsed twice with 4 ml DW , placed in 20 ml scintillation vials (Meridian, Epsom, UK), mixed with 10 ml scintillation cocktail (Goldstar, Meridian) and radioassayed using a low-activity liquid scintillation analyser (Tri-Carb 3180 TR/SL, PerkinElmer, Beaconsfield, UK) with QuantaSmart™ software. To assess their reproducibility, the pulse-chase experiments were repeated thrice. The results of two experiments are presented in Fig. 3.

Extracellular P_i labelling of *Synechococcus* cells. Cells washed of free P_i were re-suspended in $20 \text{ ml ASW-}\text{P}_i$, supplemented with $80\text{--}160 \text{ Bq ml}^{-1}$ of $\text{H}_3^{33}\text{PO}_4$ or $\text{H}_3^{32}\text{PO}_4$ and incubated in a glass bottle under standard cultivation conditions for 1–3 h. The labelled cells were collected on $0.2 \mu\text{m}$ pore size Nuclepore filters and effluent was sampled to determine the efficiency of $^*\text{P}_i$ clearance (Supplementary Table 4). Extracellularly $^*\text{P}_i$ pre-labelled *Synechococcus* cells were washed free of residual $^*\text{P}_i$ with $20 \text{ ml ASW-}\text{P}_i$ and re-suspended in solutions appropriate for further experiments.

Retention of the accumulated P_i . $^*\text{P}_i$ pre-labelled *Synechococcus* cells were treated with enzymes (Supplementary Table 6) or re-suspended in a range of solutions (Supplementary Tables 5 and 8) using either a $0.2 \mu\text{m}$ pore size PVDF membrane spin column or a $0.2 \mu\text{m}$ pore size Nuclepore membrane filter fitted in a 13 mm diameter Swinnex filter holder. For treatments in spin columns, $0.3\text{--}0.5 \text{ ml}$ treated cells were incubated in a column, spun down at $5000 \times g$ for 1 min and washed thrice with 0.1 ml of an appropriate washing solution. The radioactivity was determined separately for the cells retained in the spin column insert and for the effluent in the collection tube. Alternatively, cells were collected on a Nuclepore membrane, washed with 10 ml of a treatment solution at a rate of $0.5\text{--}1 \text{ ml min}^{-1}$ and the radioactivity determined for the filter membrane only. The activity of the protease Proteinase K in ASW was confirmed using the PDQ protease assay (Athena Environmental Sciences, Inc., Baltimore, MD, USA). To assess their reproducibility, all experiments were repeated independently at least thrice.

Inhibition experiments. Inhibitors were dissolved in dimethyl sulfoxide (DMSO) and added to samples to a final concentration of $0.05\text{--}1 \times 10^{-4} \text{ mol l}^{-1}$ (Supplementary Table 7) simultaneously with the $^{33}\text{P}_i$ or $^{32}\text{P}_i$ tracer. To provide a control, samples were supplemented with the appropriate amount of DMSO. Accumulation of $^*\text{P}_i$ in DMSO-amended samples and control samples without DMSO addition was similar (Shapiro–Wilk normality test passes $P = 0.932$, paired t -test $t = -0.155$ with 8 degrees of freedom, two-tailed P -value 0.881). Samples were incubated in the light under ambient conditions and sub-samples were withdrawn periodically to determine the total microbial P_i accumulation. To assess their reproducibility, all experiments were repeated independently at least thrice.

Microbeam synchrotron X-ray fluorescence analysis. These measurements were performed at the Diamond Light Source, the UK National Synchrotron Facility. Beamline I18 (Microfocus Spectroscopy) was used to measure the amount of P in cells of *Prochlorococcus* cyanobacteria (range $1\text{--}5 \times 10^5$ cells) and *Synechococcus* sp. strain WH8102 ($0.1\text{--}1 \times 10^6$ cells) (Supplementary Table 3). Cells were flow-sorted onto $0.2 \mu\text{m}$ pore size polycarbonate filters (P free) using the custom-built MoFlo XDP instrument⁶⁸. The filters with dried sorted cells were mounted on a custom-made sample holder and the cell-containing filter areas ($\sim 1000 \times 2000 \mu\text{m}$) were probed with a beam spot of $30 \times 30 \mu\text{m}^2$ in a helium atmosphere (Supplementary Fig. 3a–c). An approximation of the number of photons on the sample was derived by measuring a thin-film reference material with known mass deposition of a number of metals. This calculated photon flux applied to the cells and accounting for differences in sample matrix, density and volume, leads to an estimated P mass per pixel for the cells. From these values, the total number of P atoms was derived for each cell preparation by integrating signal from all P containing pixels using PyMCA X-ray Fluorescence Toolkit (<http://pymca.sourceforge.net>) and ImageJ 1.50i (<https://imagej.nih.gov/ij/>). Using the cultured *Synechococcus* cells as calibrants, sensitivity ($\geq 2 \times 10^4$ cells) and linear range ($\leq 7.5 \times 10^5$) of the method were determined.

The determined P content was $4.14 \pm 1.06 \times 10^6$ P atoms per cell for oceanic *Prochlorococcus* equivalent to 1.3–3.1 genomes (accessions: ASM1148v1, ASM1246v1, ASM1264v1, ASM1564v1, ASM1566v1, ASM1858v1, ASM75985v1, ASM792v1 and ASM1146v1). The extracellularly accumulated P_i of cells was removed during sorting by the sheath fluid of low osmotic concentration ($\sim 0.03 \text{ osmol l}^{-1}$), which strips the extracellularly bound P_i (Figs. 1, 3, and 5–7). Therefore, only intracellular phosphorus was measured for the sorted cells. In comparison, the P content calculated for an exponentially growing extracellular P_i -free *Synechococcus* sp. WH8102 cell was $1.9 \pm 0.16 \times 10^7$ P atoms, which is ~ 4 times the genomic P content (ASM19597v1).

Microscopy. Bacterioplankton cells were imaged and their dimensions measured⁶⁸ (Supplementary Fig. 3d–f and Supplementary Table 1). Cells of *Synechococcus* sp. WH8102 were imaged using a LSM780 Confocal Laser Scanning Microscope (Carl Zeiss, Jena, Germany), using 488 nm (Ar) and 594 nm (HeNe) laser lines.

Statistics and reproducibility. Each experiment was repeated independently at least three times and often more than ten times.

Reporting summary. Further information on research design is available in the Nature Research Reporting Summary linked to this article.

Data availability

The auxiliary data collected on research cruises are archived indefinitely at the British Oceanographic Data Centre (BODC) and are available at www.bodc.ac.uk. The μ -SXRF data are available from Open Science Framework at <http://osf.io/6RH2V>. All other data supporting the findings of this study are available within the paper and its Supplementary Information files. The source data underlying Figs. 2–4 and 6–9, and Supplementary Figs. 2, 4 and 5 are provided as a Source Data file.

Received: 12 February 2019; Accepted: 24 April 2020;

Published online: 26 May 2020

References

- Moore, L. R., Ostrowski, M., Scanlan, D. J., Feren, K. & Sweetsir, T. Ecotypic variation in phosphorus acquisition mechanisms within marine picocyanobacteria. *Aquat. Microb. Ecol.* **39**, 257–269 (2005).
- Sohm, J. A. & Capone, D. G. Phosphorus dynamics of the tropical and subtropical north Atlantic: *Trichodesmium* spp. versus bulk plankton. *Mar. Ecol. Prog. Ser.* **317**, 21–28 (2006).
- Dyhrman, S. T. & Haley, S. T. Phosphorus scavenging in the unicellular marine diazotroph *Crocospaera watsonii*. *Appl. Environ. Microbiol.* **72**, 1452–1458 (2006).
- Van Mooy, B. A., Rocap, G., Fredricks, H. F., Evans, C. T. & Devol, A. H. Sulfolipids dramatically decrease phosphorus demand by picocyanobacteria in oligotrophic marine environments. *Proc. Natl Acad. Sci. USA* **103**, 8607–8612 (2006).
- Mather, R. L. et al. Phosphorus cycling in the North and South Atlantic Ocean subtropical gyres. *Nat. Geosci.* **1**, 439 (2008).
- Sebastian, M. & Ammerman, J. W. The alkaline phosphatase PhoX is more widely distributed in marine bacteria than the classical PhoA. *ISME J.* **3**, 563 (2009).
- Zubkov, M. V. et al. Microbial control of phosphate in the nutrient-depleted North Atlantic subtropical gyre. *Environ. Microbiol.* **9**, 2079–2089 (2007).
- Michelou, V. K., Lomas, M. W. & Kirchman, D. L. Phosphate and adenosine-5'-triphosphate uptake by cyanobacteria and heterotrophic bacteria in the Sargasso Sea. *Limnol. Oceanogr.* **56**, 323–332 (2011).
- Gomez-Pereira, P. R. et al. Comparable light stimulation of organic nutrient uptake by SAR11 and *Prochlorococcus* in the North Atlantic subtropical gyre. *ISME J.* **7**, 603–614 (2013).
- Koch, A. L. in *Advances in Microbial Ecology* (ed. Marshall, K.C.) 37–70 (Springer, USA, 1990).
- Jumars, P. A. et al. Physical constraints on marine osmotrophy in an optimal foraging context. *Aquat. Microb. Ecol.* **7**, 121–159 (1993).
- Nikaido, H. & Vaara, M. Molecular basis of bacterial outer membrane permeability. *Microbiol. Rev.* **49**, 1–32 (1985).
- Pongprayoon, P., Beckstein, O., Wee, C. L. & Sansom, M. S. P. Simulations of anion transport through OprP reveal the molecular basis for high affinity and selectivity for phosphate. *Proc. Natl Acad. Sci. USA* **106**, 21614–21618 (2009).
- Fuszard, M. A., Wright, P. C. & Biggs, C. A. Cellular acclimation strategies of a minimal picocyanobacterium to phosphate stress. *FEMS Microbiol. Lett.* **306**, 127–134 (2010).

15. Rosenberg, H., Gerdes, R. & Chegwidden, K. Two systems for the uptake of phosphate in *Escherichia coli*. *J. Bacteriol.* **131**, 505–511 (1977).
16. Willsky, G. R. & Malamy, M. H. Characterization of two genetically separable inorganic phosphate transport systems in *Escherichia coli*. *J. Bacteriol.* **144**, 356–365 (1980).
17. Lebens, M., Lundquist, P., Söderlund, L., Todorovic, M. & Carlin, N. I. The nptA gene of *Vibrio cholerae* encodes a functional sodium-dependent phosphate cotransporter homologous to the type II cotransporters of eukaryotes. *J. Bacteriol.* **184**, 4466–4474 (2002).
18. Sowell, S. M. et al. Transport functions dominate the SAR11 metaproteome at low-nutrient extremes in the Sargasso Sea. *ISME J.* **3**, 93 (2008).
19. Scanlan, D. J. et al. Ecological genomics of marine picocyanobacteria. *Microbiol. Mol. Biol. Rev.* **73**, 249–299 (2009).
20. Nezransky, A., Blus-Kadosh, I., Yerushalmi, G., Banin, E. & Opatowsky, Y. The *Pseudomonas aeruginosa* phosphate transport protein PstS plays a phosphate-independent role in biofilm formation. *FASEB J.* **28**, 5223–5233 (2014).
21. McCarren, J. et al. Inactivation of *swmA* results in the loss of an outer cell layer in a swimming *Synechococcus* strain. *J. Bacteriol.* **187**, 224–230 (2005).
22. Zubkov, M. V., Martin, A. P., Hartmann, M., Grob, C. & Scanlan, D. J. Dominant oceanic bacteria secure phosphate using a large extracellular buffer. *Nat. Commun.* **6**, 7878 (2015).
23. Temperton, B., Gilbert, J. A., Quinn, J. P. & McGrath, J. W. Novel analysis of oceanic surface water metagenomes suggests importance of polyphosphate metabolism in oligotrophic environments. *PLoS ONE* **6**, e16499 (2011).
24. Li, P. -N. et al. Nutrient transport suggests an evolutionary basis for charged archaeal surface layer proteins. *ISME J.* **12**, 2389–2402 (2018).
25. Li, W. K. W. & Dickie, P. M. Metabolic inhibition of size-fractionated marine plankton radiolabeled with amino acids, glucose, bicarbonate, and phosphate in the light and dark. *Microb. Ecol.* **11**, 11–24 (1985).
26. Spiller, H., Stallings, W. Jr, Tu, C. & Gunasekaran, M. Dependence of H⁺ exchange and oxygen evolution on K⁺ in the marine cyanobacterium *Synechococcus* sp. strain UTEX 2380. *Can. J. Microbiol.* **40**, 257–265 (1994).
27. Ikeya, T., Ohki, K., Takahashi, M. & Fujita, Y. Study on phosphate uptake of the marine cyanophyte *Synechococcus* sp. NIBB 1071 in relation to oligotrophic environments in the open ocean. *Mar. Biol.* **129**, 195–202 (1997).
28. Strahl, H. & Hamoen, L. W. Membrane potential is important for bacterial cell division. *Proc. Natl Acad. Sci. USA* **107**, 12281–12286 (2010).
29. Kendall, A. I. Bacterial metabolism. *Physiol. Rev.* **3**, 438–455 (1923).
30. Mazard, S., Wilson, W. H. & Scanlan, D. J. Dissecting the physiological response to phosphorus stress in marine *Synechococcus* isolates (Cyanophyceae). *J. Phycol.* **48**, 94–105 (2012).
31. Zubkov, M. V. Faster growth of the major prokaryotic versus eukaryotic CO₂ fixers in the oligotrophic ocean. *Nat. Commun.* **5**, 3776 (2014).
32. Mary, I. et al. Light enhanced amino acid uptake by dominant bacterioplankton groups in surface waters of the Atlantic Ocean. *FEMS Microbiol. Ecol.* **63**, 36–45 (2008).
33. Zubkov, M. V. & Sleight, M. A. Ingestion and assimilation by marine protists fed on bacteria labeled with radioactive thymidine and leucine estimated without separating predator and prey. *Microb. Ecol.* **30**, 157–170 (1995).
34. Frece, J. et al. Importance of S-layer proteins in probiotic activity of *Lactobacillus acidophilus* M92. *J. Appl. Microbiol.* **98**, 285–292 (2004).
35. Parsot, C., Ménard, R., Gounon, P. & Sansonetti, P. J. Enhanced secretion through the *Shigella flexneri* Mxi-Spa translocon leads to assembly of extracellular proteins into macromolecular structures. *Mol. Microbiol.* **16**, 291–300 (2006).
36. Brahmasha, B. An abundant cell-surface polypeptide is required for swimming by the nonflagellated marine cyanobacterium *Synechococcus*. *Proc. Natl Acad. Sci. USA* **93**, 6504–6509 (1996).
37. Martin, N. L. & Beveridge, T. J. Gentamicin interaction with *Pseudomonas aeruginosa* cell envelope. *Antimicrob. Agents Chemother.* **29**, 1079–1087 (1986).
38. Masschalck, B. & Michiels, C. W. Antimicrobial properties of lysozyme in relation to foodborne vegetative bacteria. *Crit. Rev. Microbiol.* **29**, 191–214 (2003).
39. Heppel, L. A. Selective release of enzymes from bacteria. *Science* **156**, 1451–1455 (1967).
40. Martiny, A. C., Coleman, M. L. & Chisholm, S. W. Phosphate acquisition genes in *Prochlorococcus* ecotypes: evidence for genome-wide adaptation. *Proc. Natl Acad. Sci. USA* **103**, 12552–12557 (2006).
41. Tetu, S. G. et al. Microarray analysis of phosphate regulation in the marine cyanobacterium *Synechococcus* sp. WH8102. *ISME J.* **3**, 835–849 (2009).
42. Luecke, H. & Quijoch, F. A. High specificity of a phosphate transport protein determined by hydrogen bonds. *Nature* **347**, 402–406 (1990).
43. Scanlan, D. J. & West, N. J. Molecular ecology of the marine cyanobacterial genera *Prochlorococcus* and *Synechococcus*. *FEMS Microbiol. Ecol.* **40**, 1–12 (2002).
44. Palenik, B. et al. The genome of a motile marine *Synechococcus*. *Nature* **424**, 1037–1042 (2003).
45. Martinez, J. & Azam, F. Aminopeptidase activity in marine Chroococcoid cyanobacteria. *Appl. Environ. Microbiol.* **59**, 3701–3707 (1993).
46. Hobot, J. A., Carlemalm, E., Villiger, W. & Kellenberger, E. Periplasmic gel: new concept resulting from the reinvestigation of bacterial cell envelope ultrastructure by new methods. *J. Bacteriol.* **160**, 143–152 (1984).
47. Ting, C. S., Hsieh, C., Sundaraman, S., Mannella, C. & Marko, M. Cryo-electron tomography reveals the comparative three-dimensional architecture of *Prochlorococcus*, a globally important marine cyanobacterium. *J. Bacteriol.* **189**, 4485–4493 (2007).
48. Sanudo-Wilhelmy, S. A. et al. The impact of surface-adsorbed phosphorus on phytoplankton Redfield stoichiometry. *Nature* **432**, 897–901 (2004).
49. Fu, F.-X., Zhang, Y., Feng, Y. & Hutchins, D. A. Phosphate and ATP uptake and growth kinetics in axenic cultures of the cyanobacterium *Synechococcus* CCMP 1334. *Eur. J. Phycol.* **41**, 15–28 (2006).
50. Walter, J. M., Greenfield, D., Bustamante, C. & Liphardt, J. Light-powering *Escherichia coli* with proteorhodopsin. *Proc. Natl Acad. Sci. USA* **104**, 2408–2412 (2007).
51. Scholes, P., Mitchell, P. & Moyle, J. The polarity of proton translocation in some photosynthetic microorganisms. *Eur. J. Biochem.* **8**, 450–454 (1969).
52. Nitschmann, W. H. & Peschke, G. A. Oxidative phosphorylation and energy buffering in cyanobacteria. *J. Bacteriol.* **168**, 1205–1211 (1986).
53. Belkin, S. & Packer, L. Determination of pH gradients in intact cyanobacteria by electron spin resonance spectroscopy. *Methods Enzymol.* **167**, 670–677 (1988).
54. Marion, G. M. et al. pH of seawater. *Mar. Chem.* **126**, 89–96 (2011).
55. Padan, E. & Schuldiner, S. Molecular physiology of Na⁺/H⁺ antiporters, key transporters in circulation of Na⁺ and H⁺ in cells. *Biochim. Biophys. Acta Bioenerg.* **1185**, 129–151 (1994).
56. Dufresne, A. et al. Genome sequence of the cyanobacterium *Prochlorococcus marinus* SS120, a nearly minimal oxyphototrophic genome. *Proc. Natl Acad. Sci. USA* **100**, 10020–10025 (2003).
57. Atlas, E., Culberson, C. & Pytkowicz, R. M. Phosphate association with Na⁺, Ca²⁺ and Mg²⁺ in seawater. *Mar. Chem.* **4**, 243–254 (1976).
58. Dickson, A. G. & Riley, J. P. The estimation of acid dissociation constants in sea-water media from potentiometric titrations with strong base. II. The dissociation of phosphoric acid. *Mar. Chem.* **7**, 101–109 (1979).
59. Skulachev, V. P. The sodium cycle: a novel type of bacterial energetics. *J. Bioenerg. Biomembr.* **21**, 635–647 (1989).
60. Müller, V. & Grüber, G. ATP synthases: structure, function and evolution of unique energy converters. *Cell Mol. Life Sci.* **60**, 474–494 (2003).
61. Rojas, E. R. et al. The outer membrane is an essential load-bearing element in Gram-negative bacteria. *Nature* **559**, 617 (2018).
62. Martin, W. & Russell, M. J. On the origins of cells: a hypothesis for the evolutionary transitions from abiotic geochemistry to chemoautotrophic prokaryotes, and from prokaryotes to nucleated cells. *Philos. Trans. R. Soc. B* **358**, 59–85 (2003).
63. Zwirgmaier, K. et al. Basin-scale distribution patterns of picocyanobacterial lineages in the Atlantic Ocean. *Environ. Microbiol.* **9**, 1278–1290 (2007).
64. Post A. F. in *Harmful Cyanobacteria* (eds Huisman, J., Matthijs, H. C. P. & Visser, P. M.) Ch. 5 (Springer, 2005).
65. Mazard, S., Ostrowski, M., Partensky, F. & Scanlan, D. J. Multi-locus sequence analysis, taxonomic resolution and biogeography of marine *Synechococcus*. *Environ. Microbiol.* **14**, 372–386 (2012).
66. Farrant, G. K. et al. Delineating ecologically significant taxonomic units from global patterns of marine picocyanobacteria. *Proc. Natl Acad. Sci. USA* **113**, E3365–E3374 (2016).
67. Sohm, J. A. et al. Co-occurring *Synechococcus* ecotypes occupy four major oceanic regimes defined by temperature, macronutrients and iron. *ISME J.* **10**, 333–345 (2016).
68. Kamennaya, N. A., Kennaway, G., Fuchs, B. M. & Zubkov, M. V. “Pomacytosis”—Semi-extracellular phagocytosis of cyanobacteria by the smallest marine algae. *PLoS Biol.* **16**, e2003502 (2018).
69. Zubkov, M. V., Burkill, P. H. & Topping, J. N. Flow cytometric enumeration of DNA-stained oceanic planktonic protists. *J. Plankton Res.* **29**, 79–86 (2007).
70. Marie, D., Partensky, F., Jacquet, S. & Vault, D. Enumeration and cell cycle analysis of natural populations of marine picoplankton by flow cytometry using the nucleic acid stain SYBR Green I. *Appl. Environ. Microbiol.* **63**, 186–193 (1997).
71. Hartmann, M. et al. Efficient CO₂ fixation by surface *Prochlorococcus* in the Atlantic Ocean. *ISME J.* **8**, 2280 (2014).
72. Scanlan, D. J., Mann, N. H. & Carr, N. G. The response of the picoplanktonic marine cyanobacterium *Synechococcus* species WH7803 to phosphate starvation involves a protein homologous to the periplasmic phosphate-binding protein of *Escherichia coli*. *Mol. Microbiol.* **10**, 181–191 (1993).

Acknowledgements

We thank the captains, officers, crew and chief scientists of the research cruises JCR091, MSM03, JC053, JC079 and DY084. We are grateful to M. A. Sleight and D. Green for their supportive criticism of earlier versions of the manuscript, to J. Wulf, I. Mary, C. Grob and M. Hartmann for help with experiments at sea, and to H. Zer for help with the biochemical analysis. This study was supported by the UK Natural Environment Research Council through Research grants NE/M014363/1 and NE/J02273X/1. We acknowledge the Diamond Light Source for beam time under proposal NT15802-1.

Author contributions

M.V.Z. and N.A.K. conceived the project, designed and performed the experiments, analysed and interpreted the data and co-wrote the manuscript. K.G. designed and performed μ -XRF phosphorus measurements and analysed data. D.J.S. contributed expert advice. M.V.Z. and D.J.S. provided funding. All authors critically edited the manuscript.

Competing interests

The authors declare no competing interests.

Additional information

Supplementary information is available for this paper at <https://doi.org/10.1038/s41467-020-16428-w>.

Correspondence and requests for materials should be addressed to M.V.Z.

Peer review information *Nature Communications* thanks Adam Martiny, and the other, anonymous, reviewer(s) for their contribution to the peer review of this work.

Reprints and permission information is available at <http://www.nature.com/reprints>

Publisher's note Springer Nature remains neutral with regard to jurisdictional claims in published maps and institutional affiliations.



Open Access This article is licensed under a Creative Commons Attribution 4.0 International License, which permits use, sharing, adaptation, distribution and reproduction in any medium or format, as long as you give appropriate credit to the original author(s) and the source, provide a link to the Creative Commons license, and indicate if changes were made. The images or other third party material in this article are included in the article's Creative Commons license, unless indicated otherwise in a credit line to the material. If material is not included in the article's Creative Commons license and your intended use is not permitted by statutory regulation or exceeds the permitted use, you will need to obtain permission directly from the copyright holder. To view a copy of this license, visit <http://creativecommons.org/licenses/by/4.0/>.

© The Author(s) 2020